Electronic properties of 2D and 3D hybrid organic/inorganic perovskites for optoelectronic and photovoltaic applications

Laurent Pedesseau, Jean-Marc Jancu, Alain Rolland, Emmanuelle Deleporte, Claudine Katan, Jacky Even

Electronic properties of 2D and 3D hybrid organic/inorganic perovskites for optoelectronic and photovoltaic applications

LAURENT PEDESSEAU[1,*], JEAN-MARC JANCU[1], ALAIN ROLLAND[1], EMMANUELLE DELEPORTE[2], CLAUDINE KATAN[3], AND JACKY EVEN[1] .

[1]*Université Européenne de Bretagne, INSA Rennes, CNRS, UMR 6082 FOTON-OHM, 20 avenue des Buttes de Coësmes 35708 Rennes, France*

[2]*Laboratoire de Photonique Quantique et Moléculaire, Ecole Normale Supérieure de Cachan, 61 Avenue du Président Wilson, 94 235 Cachan Cedex, France*

[3] *CNRS, Institut des Sciences Chimiques de Rennes, UMR 6226, 35042 Rennes, France*

*(*author for correspondence: E-mail: laurent.pedesseau@insa-rennes.fr)*

Abstract. We herein investigate theoretically both 2D and 3D Hybrid Organic/inorganic Perovskite (HOP) crystal structures based on Density Functional Theory (DFT) calculations and symmetry analyses. Our findings reveal the universal features of the electronic band structure for the class of lead-halide hybrids $(R\text{-}NH_3)_nPbX_m$, where (n,m)=(2,4) and (1,3) respectively for 2D and 3D structures. Among those, the large spin-orbit coupling acting on the conduction band is shown to play a major role on the band gap of these materials. Moreover, this approach can easily be generalized to related layered and 3D hybrids, thus providing a clear-sighted inside in their electronic and optical properties.

Keywords*:* Organic-inorganic perovskite semiconductors, Density functional theory, optoelectronic properties, photovoltaic, exciton

1. Introduction

Over the past decade, Hybrid Organic/inorganic Perovskites (HOP) have attracted increasing interest in the field of optoelectronics (Mitzi *et al.* 1995) and solar cells (Lee *et al.* 2012), thanks to their ease of synthesis that opens the way to low-cost technologies. Moreover, the organic part allows tailoring their optical properties by chemical substitution, leading for example to higher luminescence efficiencies and a fine tuning of emission wavelength (Zhang *et al.* 2009). Most of the recent work has focused on lead-halide based materials of general formulae $(R\text{-}NH_3)_nPbX_m$, where R is an organic group and X a halogen atom. Control of the stoichiometry (n,m) affords crystal packing of various dimensionalities, ranging from three-dimensional (3D) corner-shared perovskite lattices to 0D structures with isolated inorganic octahedra (Mercier *et al.* 2009). The quantum and dielectric confinement expected in the 2D layered HOPs (n=2,m=4) prompt active research to develop optoelectronic devices with enhanced performances (Mitzi *et al.* 1995). Indeed, such layered structures have been demonstrated to show enhanced non-linear optical properties in microcavities (Wei *et al.* 2012). More recently, 3D HOPs (n=1, m=3), with relatively small organic cations, have been suggested as a novel class of low-cost materials for high efficiency hybrid semiconductor photovoltaic cells (HSPC) (Kojima *et al.* 2009; Lee *et al.* 2012; Park 2013; Burschka *et al.* 2013).

Given the versatility offered by the organic part, the design of novel devices with enhanced responses may greatly benefit from a realistic modeling of these HOPs. Such knowledge can be gained from Density

Functional Theory (DFT) based simulations. Surprisingly, despite the important relativistic effects expected for lead, the effect of spin-orbit coupling (SOC) has been overlooked (Burschka *et al.* 2013; Sourisseau *et al.* 2007) until recently. In fact, in two recent papers by some of us, we have demonstrated the importance of SOC both for 2D (Even *et al.* 2012) and 3D (Even *et al.* 2013) lead-halide based HOPs. The present work aims to generalize our findings using related 2D and 3D structures and compare their properties, especially in terms of optical activity. To this end, we consider two structures for 2D HOPs, namely the orthorhombic and monoclinic phases of $(C_5H_{14}N^+)_2(PbI_4^{2-})$ (Billing *et al.* 2007) and $(C_2H_7IN^+)_2(PbI_4^{2-})$ (Sourisseau *et al.* 2007) respectively (Fig. 1), and one for the 3D HOPs, namely the low temperature orthorhombic phase of $(CH_3NH_3)PbI_3$ (Baikie *et al.* 2013), hereafter abbreviated to $MAPbI_3$. We mention that while numerous self-assembled HOP (SAHOP) systems with lead-halides have been studied, only a few related crystallographic structures are known precisely. In fact, growth of monocrystals for X-ray diffraction is difficult because of the lattice disorder and strain induced by the organic molecule that however plays a fundamental role in the dielectric confinement of 2D HOPs. Nevertheless, we believe that this study will contribute to reach the level of knowledge already attained for conventional semiconductors that will be used as a reference.

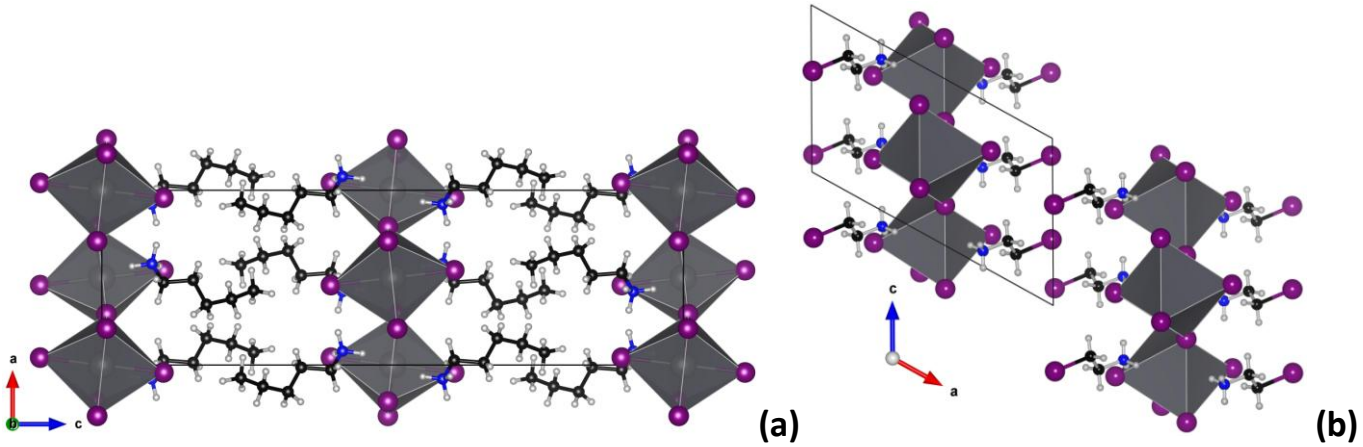

Fig. 1. Orthorhombic and monoclinic crystal structures of $(C_5H_{14}N^+)_2(PbI_4^{2-})$ (a) and $(C_2H_7IN^+)_2(PbI_4^{2-})$ (b), respectively.

2. Computational details

All DFT calculations were performed with the ABINIT package (Gonze *et al.* 2002) or VASP code (G. Kresse and J. Furthmüller, Phys. Rev. B 54, 11169 (1996).). For both 2D HOPs, we employed the LDA or the PBE gradient correction for exchange-correlation (Perdew *et al.* 1996) to ensure appropriate comparison to earlier results on $(pFC_8H_{12}N^+)_2(PbI_4^{2-})$ (Even *et al.* 2012) and $MAPbI_3$ (Even *et al.* 2013). For the latter compound, additional band structure calculations were carried out within the Local Density Approximation (LDA) on the low-temperature orthorhombic phase. A plane-wave basis set with an energy cutoff of 950 eV was used to expand the electronic wave-functions. The reciprocal space integration was performed over 4 × 4 × 4 and 4 × 4 × 1 Monkhorst−Pack grids (Monkhorst and Pack 1976) for $MAPbI_3$, $(C_5H_{14}N^+)_2(PbI_4^{2-})$ and $(C_2H_7IN^+)_2(PbI_4^{2-})$, respectively. Energies were computed from the linear response method and convergence was accurately checked with tolerance on the residual potential that stems from differences between the input and output potentials. To reveal the importance of SOC, calculations were carried out both with and without SOC and relativistic norm conserving separable dual-space Gaussian type pseudopotentials (Hartwigsen *et al.* 1998) were employed. This approach was already checked for HOP crystals against all-electron computations (Even *et al.* 2013).

3. 2D lead halide HOPs

The electronic band structure calculated without SOC of $(C_5H_{14}N^+)_2(PbI_4^{2-})$ and $(C_2H_7IN^+)_2(PbI_4^{2-})$ are shown Fig.2 (a) and (b) respectively. For the monoclinic phase of $(C_2H_7IN^+)_2(PbI_4^{2-})$, the optical absorption near the band-edge involves three active Bloch states at the Γ-point: a non-degenerate level for the VB maximum (VBM) and two nearly doubly-degenerate levels for the CB minimum (CBM). This is consistent with the band structure reported for the monoclinic phase of $(pFC_8H_{12}N^+)_2(PbI_4^{2-})$ (Even *et al.* 2012). For the orthorhombic phase of $(C_5H_{14}N^+)_2(PbI_4^{2-})$, the number of electronic states involved at the CBM and VBM is twice larger but still degenerated, due to the unit cell doubling along the stacking axis. Nevertheless, this cell doubling has no direct consequences on properties since inorganic layers are electronically decoupled. Indeed, as shown Fig 2(a), no dispersion can be seen along the Γ-Z direction (corresponding to the stacking axis in real space) even though $(C_5H_{14}N^+)_2(PbI_4^{2-})$ is one of the HOPs with the shortest aliphatic chain (Fig.1 (a)) (Lemmerer *et al.* 2012). This 2D confinement is a direct consequence of the dielectric mismatch between PbI_4 anionic layers and the organic cationic sheets (Even *et al.* 2012). As a result, the density of states close to the band gap exhibits a reduced 2D dimensionality in connection with the 2D character of excitons reported for related SAHOPs (Hong *et al.* 1992). Interestingly, the band structure of $(C_2H_7IN^+)_2(PbI_4^{2-})$ (Fig. 2(b)) reveals small dispersions of the band edge states along the Γ-Y direction (corresponding to the stacking axis in real space). This effect is rarely observed in the simulations of the electronic properties of 2D HOPs. In fact, the $(C_2H_7IN^+)_2(PbI_4^{2-})$ crystal structure exhibits a particular feature (Fig.1 (b)): the iodoethylammonium cations are organized so as to form a sheet of iodine atoms intercalated between the layers. The small dispersion observed along Γ-Y may thus be the consequence of a reduced dielectric mismatch between the sheets and a weak coupling between inorganic layers.

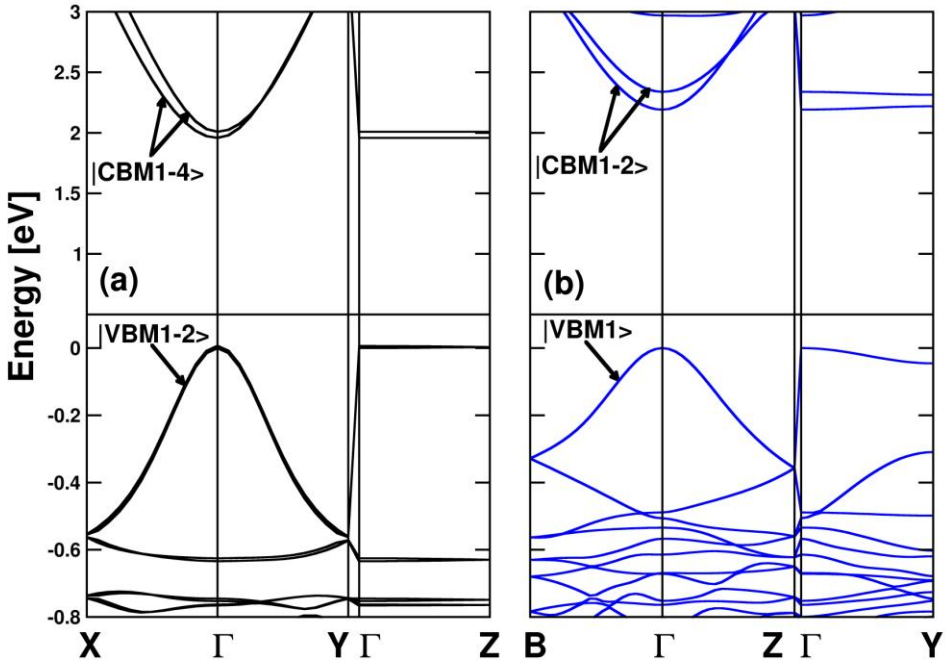

Fig. 2. Electronic band structures of the $(C_5H_{14}N^+)_2(PbI_4^{2-})$ (a) and $(C_2H_7IN^+)_2(PbI_4^{2-})$ (b) compounds without SOC calculated at the GGA PBE level. The origin of the energy scale is taken at the top of the VB.

Moreover, the DFT band structures reveal a direct band-gap that is preserved when taking SOC into account (Fig. 3). The direct character of the fundamental transition is consistent with the luminescence reported at room temperature for related SAHOPs [2]. For $(C_5H_{14}N^+)_2(PbI_4^{2-})$, the calculated band gaps amounts to 2.0 and 1.2 eV, respectively without (Fig. 2(a)) and with SOC (Fig. 3). Similarly to earlier findings on

$(pFC_8H_{12}N^+)_2(PbI_4^{2-})$, it evidences a large spin-orbit split-off of the first CB levels (1.2eV) that cannot be reasonably disregarded. Direct comparison to experimental band gaps is hampered due to the well-known underestimation afforded by ground state DFT computations. Including many-body effects, by means of GW self-energy correction for the band gap or resolution of the Bethe Salpeter equation for the excitons, may cure this problem. Unfortunately, such calculations are beyond available computational resources for these large crystal structures. However, the one-shot GW self-energy correction of +0,6eV reported for the cubic phase of $CsPbI_3$ (Even *et al.* 2013) is a clear indication that GW corrections should be large and act in the opposite direction to the SOC effect that reduces the band gaps red. Thus, we underline that a good agreement between experimental and DFT band gaps calculated without SOC is fortuitous and a consequence of error compensations. Despite this shortcoming, the overall conclusions related to the energy band dispersions and symmetries are reliable and can be used to build semi-empirical Hamiltonians, such as a **k.p** model, where detailed information of Bloch states and selection rules are required, or inspect the band gap changes related to phase transitions.

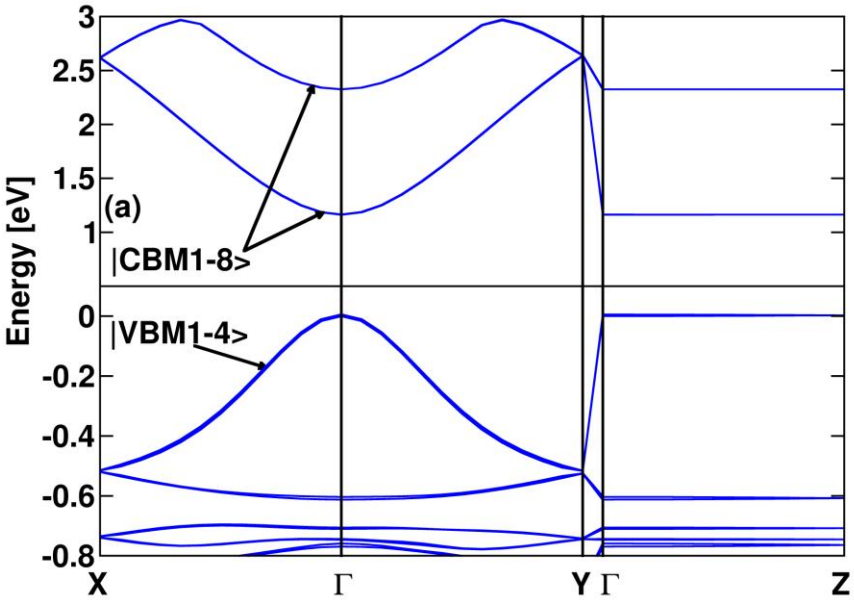

Fig. 3. Electronic band structures of $(C_5H_{14}N^+)_2(PbI_4^{2-})$ with SOC calculated at the GGA PBE level. The origin of the energy scale is taken at the top of the VB.

In fact, the calculated band gap change when going from the monoclinic low temperature phase (293K) to the orthorhombic high temperature phase (334K) of $(C_5H_{14}N^+)_2(PbI_4^{2-})$ amounts to 0.15eV both with and without SOC. This band gap reduction is consistent both with the color change from orange to red reported by Billing and Lemmerer and with that reported on a C_{12}-alkylammonium.

Overall, the present results on $(C_5H_{14}N^+)_2(PbI_4^{2-})$ and $(C_2H_7IN^+)_2(PbI_4^{2-})$ confirm the general conclusions drawn from the study of the reference compound $(pFC_8H_{12}N^+)_2(PbI_4^{2-})$ (Even *et al.* 2012). The fundamental transition of these 2D lead halide HOPs displays a nearly-perfect transverse electric character (TE). This TE character might be further enhanced in SAHOP thanks to orientational disorder introduced by the organic part. It is similar to that reported for conventional zinc-blende quantum wells with D_{2d} point symmetry or anisotropic würtzite crystals having C_{6v} point symmetry. However, symmetry and ordering of the Bloch states are reversed between the HOPs and the tetrahedrally bonded conventional semiconductors. This is also the case for the SOC splitting that acts on the CB in HOPs while it splits VB in conventional semiconductors. Pushing further the analogy with conventional semiconductors, one can define Kane matrix elements ($P_{ij}= \hbar M_{VBMi,CBMj}/m_e$, where $M_{VBMi,CBMj}$ is the dipolar matrix elements between states VBMi and CBMj) and derive

corresponding Kane energies. For III-V semiconductors, the Kane energy E_{11} is about 20eV and excitons have low binding energies of a few meV, typical for extended Wannier-Mott excitons. In contrast, the Kane energy of the present 2D HOPs is four times smaller and excitons are strongly bound, given the large binding energies of a few hundreds of meV reported in related SAHOP (Hong *et al.* 1992). We believe that both the exciton's binding energy and the Kane energy are at the origin of the peculiar optical properties of this class of materials.

4. 3D versus 2D lead halide HOPs

Contrarily to the 2D hybrids, 3D HOPs show sizeable dispersion in the whole Brillouin zone as illustrated Fig. 4. Therefore, theory predicts an almost isotropic absorption for these materials. The direct band gap at the center of the Brillouin zone is consistent with the strong absorbance reported at room temperature (Tanaka *et al.* 2003; Lee *et al.* 2012). The fundamental transitions for the low temperature phase of $MAPbBr_3$ calculated at the GGA level of theory amount to 2.0 eV (Fig. 4 (a)) without SOC with VASP code. Identically, the fundamental transitions for the low temperature phase (T<161K) (Baikie *et al.* 2013) of $MAPbI_3$ calculated at the GGA level of theory amount to 1.6 eV (Fig. 4 (b)) and 0.7 (Fig. 4 (c)) respectively without and with SOC with VASP code. These values confirmed the large effect of SOC (Even *et al.* 2013). Moreover, the splitting is large and comparable to that calculated for the 2D lead halide HOPs. These theoretical results are consistent with the SOC effects revealed in optical reflectivity (Hirasawa *et al.* 1994) and absorption (Tanaka *et al.* 2003) measurements on $MAPbI_3$. Thus, the same conclusion holds regarding SOC inclusion for relevant band structure calculations on such materials. In addition, as for the 2D HOPs, accurate prediction of absolute band gaps of these 3D analogues requires also many-body technics whereas both dispersions and symmetry considerations stay reliable on the DFT level of theory.

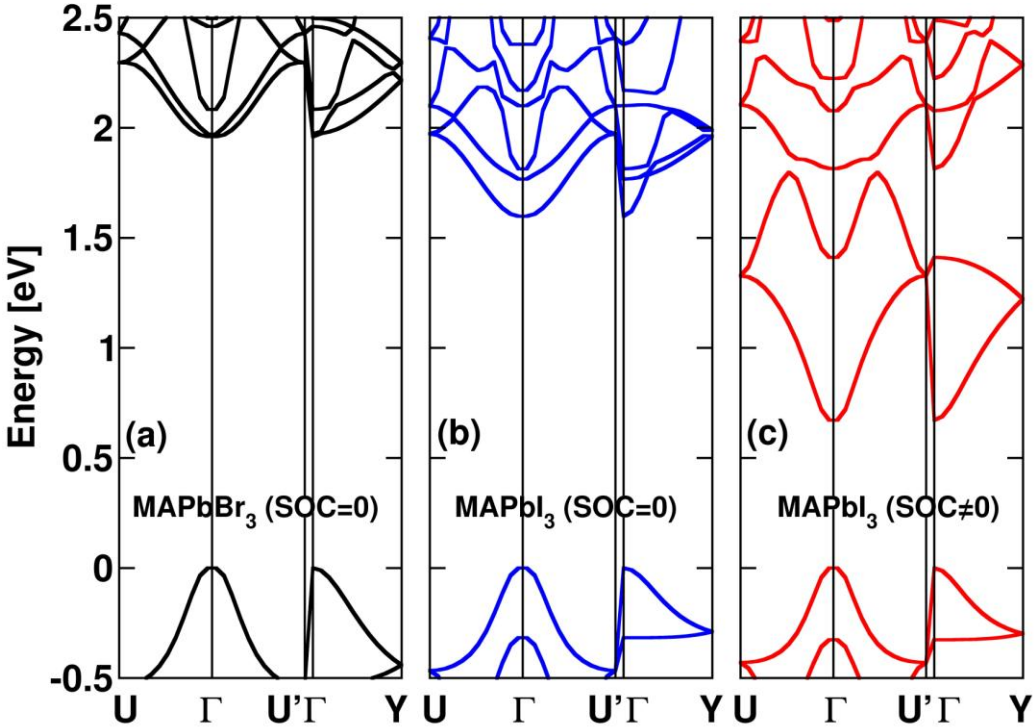

Fig. 4. Electronic band structures of $MAPbBr_3$ without (a) SOC, $MAPbI_3$ without (b) and with (c) SOC calculated at the GGA level. The origin of the energy scale is taken at the top of the VB.

Among the noticeable differences between 2D and 3D lead-halide HOPS considered in this work, strain effects induce a splitting of the VBM in the latter (Fig. 4). Strain effects act also on the CBM but the splitting

introduced by SOC effects is much larger leading to comparable band gap reductions in both 2D and 3D HOPs. The high temperature (T>330K) phase of $MAPbI_3$ is cubic and the room temperature phase is a slightly distorted tetragonal phase (Baikie *et al.* 2013). The analysis of critical electronic states most relevant for applications can indeed be performed using the cubic phase as a reference (Even *et al.* 2013). When SOC is not taken into account, the cubic phase has a triply-degenerated CB associated to the vectorial representation of a cubic simple group, commonly described by the $|X\rangle$, $|Y\rangle$, $|Z\rangle$ symbols. For the low temperature orthorhombic phase considered here, the number of CB states is doubled (Fig. 4 (b)). In the corresponding double group including spinors, the CB of the high temperature cubic phase gets split by SOC into twofold degenerate states and fourfold degenerate states (Even *et al.* 2013). A similar effect is predicted for the low-temperature phase although strain effects must be taken into account for a detailed analysis (Fig. 4 (c)). The high (and room) temperature CBM is associated to the twofold degenerate spin-orbit split-off states

$$|1/2,1/2\rangle = \frac{1}{\sqrt{3}}|(X+iY)\uparrow\rangle + \frac{1}{\sqrt{3}}|Z\downarrow\rangle$$

and

$$|1/2,-1/2\rangle = \frac{1}{\sqrt{3}}|(X-iY)\downarrow\rangle + \frac{1}{\sqrt{3}}|Z\uparrow\rangle$$

These spin-orbit split-off states lead to strong and isotropic optical transitions with the even $|S\rangle$-like VBM states. We underline that for both 2D and 3D HOPs, one obtains reversed ordering of band-edge states as compared to tetrahedrally bonded conventional semiconductors.

In 3D crystals, strain effects induce an additional contribution to splitting on the conduction bands. For both types of HOPs, the calculated band gap is direct in agreement with strong absorbance or luminescence observed at room temperature. The electronic band structure of 2D hybrids reveals effectively the 2D character with none or little dispersion in the direction of reciprocal space corresponding to the layers staking axis, depending on the nature of the cationic layer that may affect the dielectric contrast between organic and inorganic sheets. The fundamental transitions have a nearly perfect transverse electric character, similarly to zinc-blende quantum wells or würtzite bulk compounds with respectively D_{2d} or C_{6v} point symmetry. In contrast, for 3D hybrids almost isotropic optical activity is expected from symmetry. Indeed, for the high temperature cubic phase, this activity stems from transitions between a triply degenerated conduction-band and a single valence-band, in a simple group representation. In the double group representation, the resulting twofold degenerate spin-orbit split-off states are build from a weighted mixture of these conduction band states that retain the isotropic nature of the optical activity.

5. Summary

Based on DFT calculations and symmetry analyses of the band-edge states, the electronic and optical properties of both 2D and 3D lead-halide hybrid perovskites have been investigated. In these materials, spin orbit effects induce a dramatic splitting of the conduction bands and appear to dominate their band gap. These results are consistent with evidence of SOC in reflectivity and absorption spectra reported earlier on $MAPbX_3$. Both types of hybrids exhibit a reversed band ordering when compared to conventional

semiconductor quantum wells and bulk materials.

Acknowledgment

This work was performed using HPC resources from GENCI CINES and IDRIS 2013-2013096724. The work is supported through the participation of the PEROCAI ANR project.

References

Mitzi, D.B., Wang, S., Field, C.A., Chess, C.A. and Guloy, A.M.: Conducting Layered Organic-inorganic Halides Containing <110>-Oriented Perovskite Sheets. Science. **267**, 1473-1476 (1995)

Lee, M. M., Teuscher, J., Miyasaka, T., Murakami, T. N. and Snaith, H. J.: Efficient Hybrid Solar Cells Based on Meso-Superstructured Organometal Halide Perovskites. Science. **338**, 643-647 (2012)

Zhang, S., Lanty, G., Lauret, J. S., Deleporte, E., Audebert, P. and Galmiche, L.: Synthesis and optical properties of novel organic–inorganic hybrid nanolayer structure semiconductors. Acta Materialia, 57, 3301-3309 (2009)

Mercier, N., Louvain, N. and Bi, W. H.: Structural diversity and retro-crystal engineering analysis of iodometalate hybrids. CrystEngComm, **11**, 720-734 (2009)

Wei, Y., Lauret, J.-S., Galmiche, L., Audebert P. and Deleporte, E.: Strong exciton-photon coupling in microcavities containing new fluorophenethylamine based perovskite compounds. Optics Express. **20**, 10399-10405 (2012)

Kojima, A.; Teshima, K.; Shirai, Y. and Miyasaka, T.: Organometal Halide Perovskites as Visible-Light Sensitizers for Photovoltaic Cells. J. Am. Chem. Soc., **131**, 6050−6051 (2009)

Park, N. G.: Organometal Perovskite Light Absorbers Toward a 20% Efficiency Low-Cost Solid-State Mesoscopic Solar Cell. J. Phys Chem. Lett. **4**, 2423-2429 (2013)

Burschka, J., Pellet, N., Moon, S.J., Humphry-Baker, R., Gao, P., Nazeeruddin, M.K. and Grätzel, M.: Sequential deposition as a route to high-performance perovskite-sensitized solar cells. Nature, **499**, 316–319 (2013)

Sourisseau, S., Louvain, N., Bi, W., Mercier, N., Rondeau, D., Boucher, F., Buzaré, J.-Y. and Legein, C.: Reduced Band Gap Hybrid Perovskites Resulting from Combined Hydrogen and Halogen Bonding at the Organic−Inorganic Interface. Chem. Mater. **19**, 600-607 (2007)

Even, J., Pedesseau, L., Dupertuis, M.-A., Jancu, J.-M. and Katan, C.: Electronic model for self-assembled hybrid organic/perovskite semiconductors: Reverse band edge electronic states ordering and spin-orbit coupling. Phys. Rev. B **86**, 205301 (2012)

Even, J., Pedesseau, L., Jancu, J.-M. and Katan, C.: Importance of Spin–Orbit Coupling in Hybrid Organic/Inorganic Perovskites for Photovoltaic Applications. J. Phys. Chem. Lett., **4**, 2999-3005 (2013)

Billing, D. G.and Lemmerer, A.: Synthesis, characterization and phase transitions in the inorganic–organic layered perovskite-type hybrids $[(C_nH_{2n+1}NH_3)_2PbI_4]$, n = 4, 5 and 6. Acta Cryst. B**63**, 735-747 (2007)

Baikie, T.; Fang, Y. N.; Kadro, J. M.; Schreyer, M.; Wei, F. X.; Mhaisalkar, S. G.; Graetzel, M. and White, T. J.: Synthesis and crystal chemistry of the hybrid perovskite $(CH_3NH_3)PbI_3$ for solid-state sensitised solar cell applications. J. Mater. Chem. A, **1**, 5628−5641 (2013).

Gonze, X., Beuken, J.-M., Caracas, R., Detraux, F., Fuchs, M., Rignanese, G.-M., Sindic, L., Verstraete, M., Zerah, G., Jollet, F., Torrent, M., Roy, A., Mikami, M., Ghosez, P., Raty, J.-Y. and Allan, D.: First-principles computation of material properties: the ABINIT software project. Computational Materials Science, 25, 478-492 (2002)

Kresse G. and Furthmüller J., Phys. Rev. B **54**, 11169 (1996)

Perdew, J. P., Burke, K. and Ernzerhof, M.: Generalized Gradient Approximation Made Simple. Phys. Rev. Lett. **77**, 3865-3868 (1996)

Monkhorst, H. J. and Pack, J. D.: Special points for Brillouin-zone integrations. Phys. Rev. B, **13**, 5188-5192 (1976)

Hartwigsen, C., Goedecker, S. and Hutter, J.: Relativistic separable dual-space Gaussian pseudopotentials from H to Rn. Phys. Rev. B **58** (7), 3641-3662, (1998)

Lemmerer, A. and Billing, D. G.: Synthesis, characterization and phase transitions of the inorganic–organic layered perovskite-type hybrids $[(C_nH_{2n+1}NH_3)_2PbI_4]$, n = 7, 8, 9. Dalton Trans. **41**, 1146-1157 (2012)

Hong, X., Ishihara, T. and Nurmikko, A. U.: Dielectric confinement effect on excitons in PbI_4-based layered semiconductors. Phys. Rev. B**45**, 6961-6964 (1992)

Tanaka, K., Takahashi, T., Ban, T., Kondo, T., Uchida, K., and Miura, N.: Comparative Study on the Excitons in Lead-Halide-Based Perovskite-Type Crystals $CH_3NH_3PbBr_3CH_3NH_3PbI_3$. Solid State Commun., **127**, 619−623 (2003)

Hirasawa, M., Ishihara, T. and Goto, T.: Exciton Features in 0-Dimensional, 2-Dimensional, and 3-Dimensional Networks of PbI_6 4-Octahedra. J. Phys. Soc. Jpn. **63**, 3870−3879 (1994).